Revista Brasileira de Ciência do Solo
ISSN: 0100-0683
revista@sbcs.org.br
Sociedade Brasileira de Ciência do Solo
Brasil

Arantes Camargo, Livia; Marques Júnior, José; Pereira, Gener Tadeu
MINERALOGY OF THE CLAY FRACTION OF ALFISOLS IN TWO SLOPE CURVATURES. III - SPATIAL VARIABILITY
Revista Brasileira de Ciência do Solo, vol. 37, núm. 2, 2013, pp. 295-306
Sociedade Brasileira de Ciência do Solo
Viçosa, Brasil

Available in: http://www.redalyc.org/articulo.oa?id=180226346001

DIVISÃO 1 - SOLO NO ESPAÇO E NO TEMPO

Comissão 1.1 - Gênese e morfologia do solo

MINERALOGY OF THE CLAY FRACTION OF ALFISOLS IN TWO SLOPE CURVATURES. III - SPATIAL VARIABILITY[1]

Livia Arantes Camargo[2], José Marques Júnior[3] & Gener Tadeu Pereira[4]

SUMMARY

A good knowledge of the spatial distribution of clay minerals in the landscape facilitates the understanding of the influence of relief on the content and crystallographic attributes of soil minerals such as goethite, hematite, kaolinite and gibbsite. This study aimed at describing the relationships between the mineral properties of the clay fraction and landscape shapes by determining the mineral properties of goethite, hematite, kaolinite and gibbsite, and assessing their dependence and spatial variability, in two slope curvatures. To this end, two 100 × 100 m grids were used to establish a total of 121 regularly spaced georeferenced sampling nodes 10 m apart. Samples were collected from the layer 0.0-0.2 m and analysed for iron oxides, and kaolinite and gibbsite in the clay fraction. Minerals in the clay fraction were characterized from their X-ray diffraction (XRD) patterns, which were interpreted and used to calculate the width at half height (WHH) and mean crystallite dimension (MCD) of iron oxides, kaolinite, and gibbsite, as well as aluminium substitution and specific surface area (SSA) in hematite and goethite. Additional calculations included the goethite and hematite contents, and the goethite/(goethite+hematite) [Gt/(Gt+Hm)] and kaolinite/(kaolinite+gibbsite) [Kt/(Kt+Gb)] ratios. Mineral properties were established by statistical analysis of the XRD data, and spatial dependence was assessed geostatistically. Mineralogical properties differed significantly between the convex area and concave area. The geostatistical analysis showed a greater number of mineralogical properties with spatial dependence and a higher range in the convex than in the concave area.

Index terms: iron oxides, kaolinite, gibbsite, goethite, hematite, relief.

---

[1] Part of the first author's dissertation. Received for publication on August 2, 2012 and approved on February 26, 2013.

[2] Doctoral student (FAPESP scholarship) of the postgraduate program in Agronomy (Soil Science) of FCAV/Jaboticabal, Universidade Estadual Paulista - UNESP, Via de acesso Prof. Paulo Donato Castellani, s/n. CEP 14884-900 Jaboticabal (SP), Brazil. E-mail: li_arantes@yahoo.com.br

[3] Prof. Dr., Soils and Fertilizers Department, FCAV/Jaboticabal - UNESP. E-mail: marques@fcav.unesp.br

[4] Prof. Dr., Exact Science Department, FCAV/Jaboticabal, UNESP. E-mail: genertp@fcav.unesp.br

RESUMO: *MINERALOGIA DA FRAÇÃO ARGILA DE UM ARGISSOLO EM CURVATURAS DO RELEVO. III - VARIABILIDADE ESPACIAL*

O conhecimento da distribuição dos minerais da fração argila na paisagem permite o entendimento da influência do relevo no teor e nos atributos dos minerais como goethita, hematita, caulinita e gibbsita. Buscando entender as relações entre os atributos dos minerais da fração argila e as formas da paisagem, o presente trabalho tem como objetivo caracterizar os atributos dos minerais da fração argila - goethita, hematita, caulinita e gibbsita - bem como, avaliar a variabilidade espacial dos mesmos em duas curvaturas. Uma malha de dimensão de 100 x 100 m foi delimitada em uma área caracterizada pela forma convexa e outra em uma área caracterizada pela forma côncava. As malhas possuíam espaçamento regular de 10 x 10 m e os pontos de cruzamento deste espaçamento determinaram os pontos de coleta das amostras, num total de 121 pontos amostrais georreferenciados em cada malha. Amostras para determinação dos óxidos de ferro e dos minerais caulinita e gibbsita da fração argila foram coletadas na profundidade 0,0-0,2 m. As amostras das áreas côncavas e convexas foram submetidas à separação da fração argila do solo e posteriormente ao processo de concentração dos óxidos de ferro para caracterização da hematita e goethita e ao processo de remoção dos óxidos de ferro para caracterização da caulinita e gibbsita. A caracterização dos minerais da fração argila foi realizada por reflexos da difração de raios-X. Os difratogramas foram interpretados e calculados os valores da largura a meia altura (LMA), diâmetro médio do cristal (DMC) dos óxidos de ferro e da caulinita e gibbsita e substituição isomórfica (SI) e área de superfície específica (ASE) da hematita e goethita. Foram também calculados os teores da goethita e hematita, razão goethita / (goethita+hematita) [Gt / (Gt+Hm)] e razão caulinita / (caulinita+gibbsita) [Ct / (Ct+Gb)]. Realizou-se a análise estatística a avaliação da variabilidade espacial por meio da geoestatística. Os atributos mineralógicos apresentaram diferença significativa entre as áreas convexa e côncava. Na análise geoestatística observou-se um maior número de atributos mineralógicos com dependência espacial e os maiores valores de alcance na área convexa em relação à área côncava.

Termos de indexação: óxidos de ferro, caulinita, gibbsita, goethita, hematita, relevo.

INTRODUCTION

In previous studies, Camargo et al. (2008a,b) and Camargo et al. (2013) found the spatial dependence of mineralogical properties in hematite, goethite, kaolinite and gibbsite to correlate with small variations in relief and evaluated the influence of these minerals on soil aggregates and available phosphorus. This study presents more detailed findings about the spatial dependence of clay minerals and the correlation between physical properties, providing additional information on Alfisols in 200-ha areas with representative slope curvatures. This information will be useful for future mapping of co-varied attributes of clay minerals in areas of commercial agricultural production.

The clay fraction of weathered tropical soils typically contains abundant 1:1 clay minerals, aside from iron and aluminium oxides and hydroxides. According to Schwertmann & Taylor (1989), goethite and hematite are the most frequent iron oxides in soils from tropical and subtropical regions. Some authors have studied the mineralogical features of the clay fraction in Brazilian agricultural soils. For example, Coelho & Vidal-Torrado (2003) studied kaolinite, hematite, goethite, gibbsite and anatase in the clay fraction of an Alfisol developed from sandstone of the Bauru Group, and Marques Junior & Lepsh (2000) examined an Alfisol from the same group in the region of Monte Alto, São Paulo, and found abundant contents of gibbsite and particularly of kaolinite.

Several authors have reported variations in the crystallographic attributes of iron oxides (Schwertmann & Kämpf, 1985; Schwertmann & Carlson 1994; Inda Júnior & Kämpf, 2005; Wiriyakitnateekul et al., 2007). These variations have been ascribed to the formation of iron oxides determined by the prevailing soil-environmental conditions (Schwertmann & Fischer, 1966; Torrent et al., 1982; Schwertmann & Murad, 1983; Kämpf & Curi, 2000). In fact, environmental variations are known to lead to varying degrees of crystallinity of goethite and hematite. Also, hematite tends to have more uniform properties than goethite since hematite is formed from ferrihydrite in the solid state and goethite in the soil solution, which is why the influence of the particular environmental conditions on hematite is stronger (Schwertmann, 1985; Schwertmann & Taylor 1989; Singer et al., 1998; Inda Júnior & Kämpf, 2005). Variations in mean crystallite dimension were also observed for kaolinite and gibbsite. Thus, Camargo et al. (2008a) found that the mean crystallite dimension ranged from 22 to 58 nm in kaolinite, and 79 to 99 nm in gibbsite, in a 1-ha Oxisol area.

Relief is considered an influential factor in the formation of clay minerals. Its relationship with crystallinity in these minerals has been the subject of much research. Mineralogy and auxiliary data can be useful to develop models for describing slope–hydrological processes at different spatial scales and interpreting soil properties in a geographic setting (Wilson et al., 2010). At the local scale, mineralogical differences reflect the effects of soil formation processes and of factors contributing to the formation of a landscape.

Moniz & Buol (1982) found hematite and goethite to be the predominant iron oxides in soil in most of the high and low portion, respectively, of the studied relief. Curi & Franzmeier (1984) found goethites with smaller crystallite sizes and higher kaolinite concentrations at lower positions in an Oxisol toposequence in the state of Goiás. Brito et al. (2006) reported a predominance of gibbsite in an area with a concave shape compared to another with a linear shape, containing kaolinite among the clay fraction minerals, in an Oxisol from the state of São Paulo. Campos et al. (2007) examined the influence of geomorphic surfaces in an Oxisol on the ratio of kaolinite/(kaolinite+gibbsite). Reatto et al. (2008) verified the influence of topography and hydric fluxes on the kaolinite and gibbsite contents of an Oxisol toposequence in Brazil.

Just as important as determining the mineral properties of the clay fraction is to understand their dependence and spatial variability in the landscape since this deepens the understanding of the environments of mineral formation and the cause-effect relationships between mineralogical properties and other soil characteristics. Some authors have related spatial variability in soil properties to landscape and small variations in relief (Souza et al., 2006; Campos et al., 2007). Cunha et al. (2005) demonstrated correlation between mineralogical properties, iron contents and various geomorphic surfaces.

Conventional statistical delineation has been successfully used to assess soil properties by means of straightforward sampling units located in relatively small areas that were fairly uniform in terms of soil properties. However, conventional statistics are useless when experiments involving extensive heterogeneous landscapes are required (Bishop & Lark, 2006). According to Pennock & Veldkamp (2006), advances in spatialization techniques for soil properties have facilitated the assessment of soil heterogeneity in the landscape. One of the possibilities to describe the dependence and spatial variability of soil properties is the technique of geostatistics based on semivariograms and kriging (Trangmar et al., 1985; Vieira, 2000). As shown by McBratney et al. (2003), the combined use of these techniques and the digital model of elevation provide an understanding of the distribution of soil properties and cause-effect relationships in their patterns. Oliveira Júnior et al. (2011) found spatial variability of clay mineralogy in an area of 12.88 ha and concluded that geostatistics analysis is the most indicated to determine the best patterns of soil sampling to assess these attributes.

The spatialization of the mineralogical properties of the clay fraction in the slope curvatures is a necessary preliminary step to understand the relationship between the minerals and variations in soil properties with a view to the transference of this knowledge to areas with a similar relief. Also, the large number of processable samples with geostatistics facilitates evaluation of not only spatial variability, but also mineral crystallinity - which is often neglected in conventional delineation techniques for the assessment of soil minerals (Camargo et al., 2013).

To date, few studies have been published on the spatial characterization of minerals in the clay fraction and their relationship and correlations with relief in soils with low iron content (e.g. Ultisols and Alfisols from the northern region in the Brazilian state of São Paulo),

The purpose of this study was to characterize the properties of the clay minerals goethite, hematite, kaolinite, and gibbsite, and to assess their dependence and spatial variability in slope curvatures.

MATERIAL AND METHODS

Study area

The study area was located in Catanduva, a municipality in the north-west of the state of São Paulo, Brazil, (latitude 21º 05' 57.11" S, longitude 49º 01' 02.08" W, 503 m a.l.s.). The Aw climate (Köppen classification) of the region is hot humid, tropical, with dry winters, a mean annual rainfall of 1,350 mm, a mean annual temperature of 23 ºC, maximum and minimum temperatures of 22 and 18 ºC, respectively, and average relative air humidity of 74 %. The primary vegetation is seasonal rain forest and Cerrado (Brazilian savanna). The current use is mainly for sugarcane with a green harvesting system (burning and cutting cane when still green), in use for over 20 years.

The soil parent material is sandstone from the Bauru Group, in the Adamantina Formation (IPT, 1981). This formation contains refined sediments, and according to Suguio (1973) and Castro (1989), its minerals are mostly rich in silicon and poor in iron.

The area was surveyed by aerial photography at a scale of 1:35,000, with topographic profiling, and geomorphologic and pedological field classification. The soil was classified as Typic Hapludalf (Soil Survey Staff, 1999) (Table 1). The slope curvatures were classified from field measurements as described by Troeh (1965), using an elaborate digital elevation model (DEM) (Figure 1). Two different morphological

Table 1. Physical and chemical properties of horizons A + E and Bt in the two selected areas

Hor.	Depth	Munsell color	FS	CS	Silt	Clay	pH ($CaCl_2$)	OM	SB	CEC	BS	SiO_2	Al_2O_3	Fe_2O_3
	cm	moist	——— g kg^{-1} ———					g dm^{-3}	$mmol_c$ dm^{-3}		%	——— g kg^{-1} ———		
Profile of the concave area (Typic Hapludalf)														
A+E	39	5YR 3/2	698	149	106	47	4.8	13	29	52	56	12	35	20
Bt	60	2.5YR 3/4	627	113	187	165	4,2	10	36	63	57	20	115	27
Profile of the convex area (Typic Hapludalf)														
A+E	30	5YR 3/3	773	69	112	46	4.8	15	28	53	52	13	40	30
Bt	60	2.5YR 4/4	531	42	162	265	5.5	11	32	61	54	21	110	40

Hor.: horizont; FS: fine sand; CS: coarse sand; OM: organic matter; SB: sum of bases; CEC: cation exchange capacity; BS: base saturation.

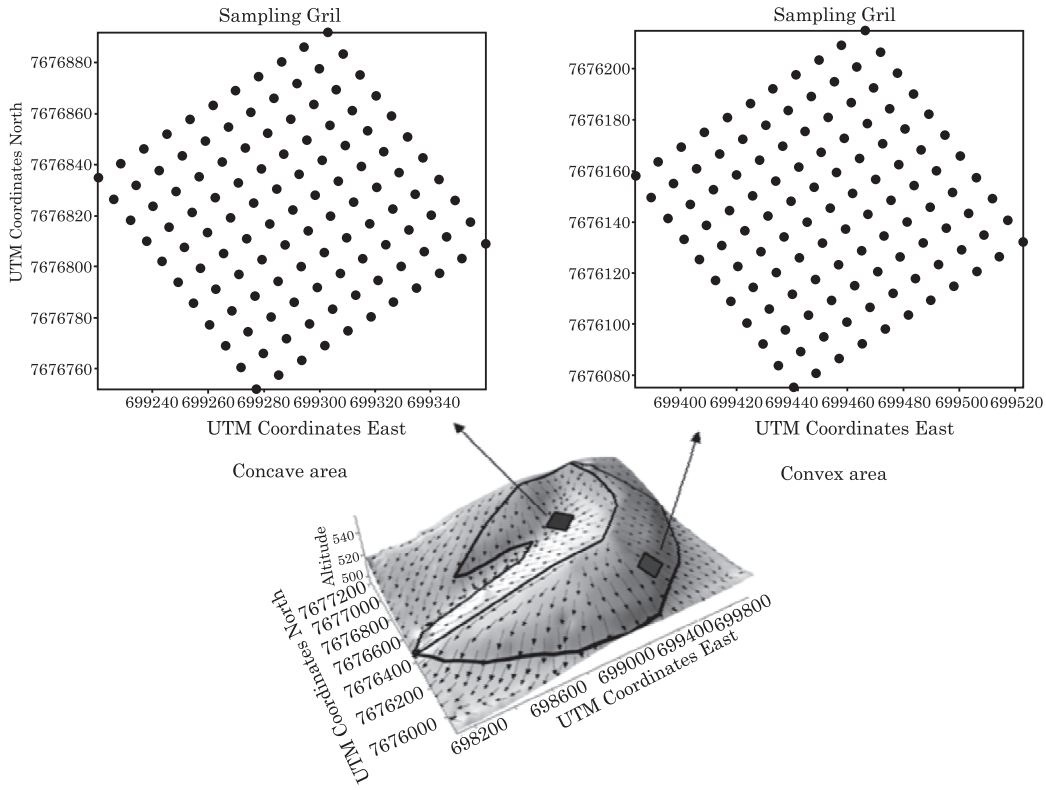

Figure 1. Digital elevation model (DEM) for the study area and sampling sites (+). The arrows in the center represent surface water flow.

areas were observed: one with convex and the other with concave slope curvatures. The annual soil loss from the convex area was 9.32 t ha^{-1} and 7.21 t ha^{-1} from the concave area.

Soil samples were collected from the 0.0-0.2 m layer at intersection points on a 100 × 100 m georeferenced grid, with regularly spaced nodes (10 x 10 m) at a representative location of each area.

Mineralogical analyses

The soil samples were treated with 0.5 mol L^{-1} NaOH under mechanical agitation for 10 min to facilitate particle dispersion. After this initial treatment, the sand fraction was sieved through a 0.05 mm mesh. Silt and clay fractions were separated by centrifugation at 1,600 rpm for a period according to the temperature of each sample at the time of analysis.

The clay suspension was flocculated with concentrated HCl and centrifuged at 2,000 rpm for 2 min. Next, iron oxides were removed from the clay fraction by extraction with dithionite-citrate-bicarbonate (DCB) according to Mehra & Jackson (1960) and analysed for kaolinite (Kt) and gibbsite (Gb).

Iron oxides and oxyhydroxides (goethite and hematite) were determined by previously concentrating the clay fraction with iron oxides, using the method of Norrish & Taylor (1961), modified by Kämpf & Schwertmann (1982).

X-ray diffraction patterns were obtained from samples prepared with the powder method, using an HGZ instrument equipped with a cobalt anode and an iron filter for hematite (Hm) and goethite (Gt) diffractions, and a copper anode with a nickel filter for Kt and Gb diffractions (Kα radiation, 20 mA, 30 kV). A scanning speed of 1º2θ per min, and an amplitude of 23-49º for hematite (012 and 110) and goethite (110 and 111), and of 11-19º for kaolinite (001) and gibbsite (002) were used.

The mean crystallite dimension (MCD) of Kt and Gb was calculated from the width at half height (WHH) and the position of the reflections for the minerals Kt (001) and Gb (002), whereas for Hm and Gt, MCD was calculated from the WHH and the positions of the Hm (110) and Gt (110) reflections. The MCD was calculated by the Scherrer equation (Schulze, 1984). Aluminium substitution (AS) in goethite was calculated from the equation proposed by Schulze (1984) and AS in hematite from an equation of Schwertmann et al. (1979).

The kaolinite/(kaolinite+gibbsite) [Kt/(Kt+Gb)] ratio was calculated from the areas for the Kt (001) and Gb (002) reflection, and the goethite/(goethite+hematite) [Gt/(Gt+Hm)] ratio from the areas for the hematite (012) and goethite (110) reflections, in the XRD patterns. The peak area for goethite (110) was multiplied by a factor of 0.35 because the intensity of the hematite (012) reflection was 35 % (Kämpf & Schwertmann, 1998). To obtain the Gt content, Fe content extracted by dithionite-citrate-bicarbonate (Mehra & Jackson, 1960) was multiplied by the ratio Gt/(Gt+Hm) and 1.59. The hematite content was determined as described by Dick (1986).

The specific surface area of goethite [SSA(Gt), $m^2\ g^{-1}$] was estimated according to Schulze & Schwertmann (1984) and that of hematite [SSA(Hm), $m^2\ g^{-1}$] according to Schwertmann & Kämpf, 1985.

$$SSA(Gt) = (1049/MCD_{100}) - 5 \quad (1)$$

where $MDC_{100} = 0.42\ MCD_{gt110}$ (nm) (Kämpf, 1981).

$$SSA(Hm) = 2\ (r+h)d \quad (2)$$

where $r = (0.71/2)\ MCD_{hm110}$; $h = 0.59\ MCD_{Hm012}$ and $d = 5.26\ g\ cm^{-3}$ (Schwertmann & Kämpf, 1985).

Statistical analyses

Experimental data were subjected to descriptive statistical analysis involving calculation of the mean, median, variance, standard deviation, asymmetry, kurtosis, maximum, minimum, coefficient of variation, and type of distribution. The differences in mean value between areas were calculated by Student's *t* test. All analyses were performed using software Minitab 14 (Minitab, 2000). The spatial variability pattern was determined by geostatistical analysis (Vieira, 2000), using GS+ from Gamma Design Software (1998), to fit the models.

RESULTS AND DISCUSSION

The analysis of the morphological properties of the two soil profiles revealed only slight differences and indicated the presence of hematite in the clay fraction, even though the Fe_2O_3 content was relatively low (20-40 g kg^{-1}) (Table 1).

Although the soils in the two areas belong to the same class, the thickness of the A+E horizon was smaller and the clay content of the Bt horizon greater in the convex area. This result can be ascribed to higher erosion from the convex than from the concave area.

The mineral properties of the grid points were subjected to a preliminary descriptive analysis (Tables 2 and 3). The hematite (Hm) and goethite (Gt) contents in the concave and convex areas are shown in table 2. Hematite was the most abundant Fe oxide, as confirmed by the low values of the goethite/(goethite+hematite) ratio [Gt/(Gt+Hm)] (Table 2).

Hematite also had the smallest width at half height (WHH) and greatest mean crystallite dimension (MCD) of the Fe oxides in both areas. In fact, its MCD was somewhat higher than that of Gt (110) (Table 2). These results are consistent with those of Fontes & Weed (1991), who found hematite to be generally more crystalline than Gt.

Aluminium substitution (AS) in Hm and Gt in both areas (Table 2) was consistent with previous results of Gualberto et al. (1987) and Inda Júnior & Kämpf (2005). However, the peak values differed. Thus, the aluminium substitution of Gt was greater and MCD smaller than Hm as a result of Fe^{3+} substitution by Al^{3+}, causing cell contraction and leading to a reduced crystallite size (Norrish & Taylor, 1961), and hence to an increased specific surface area of this mineral (Torrent et al., 1987; Schwertmann, 1991).

The specific surface area (SSA) values for the iron oxides Gt and Hm made them highly reactive to P compounds and increased their soil adsorption, resulting in plant unavailability (Peña & Torrent, 1984). However, an increased adsorption of some elements (particularly toxic ones) can be positive. Inda Júnior & Kämpf (2005) also found Gt to exhibit greater SSA values than Hm. By contrast, Schwertmann & Kämpf (1985) found smaller SSA values for Hm and Gt in similar soils. Also, Barrón et al. (1988) reported SSA values from 6 to 115 $m^2\ g^{-1}$ for synthetic hematite, and Torrent et al. (1990) found similar values for goethite. The difference can be ascribed to the use of

Table 2. Descriptive statistics of the properties of goethite and hematite in the convex and concave area

Attribute		Area	Mean	Median	Minimum	Maximum	Variance	Asymmetry	Kurtosis	SD[6]	CV (%)[7]	p[8]
WHH[1]	Gt	convex	0.52	0.53	0.30	0.83	0.008	0.08	0.50	0.08	16.79	<0.005
		concave	0.54	0.53	0.30	0.90	0.011	0.37	0.41	0.10	19.38	<0.005
	Hm	convex	0.40	0.38	0.30	0.53	0.002	0.05	0.70	0.04	10.28	<0.005
		concave	0.36	0.38	0.30	0.53	0.003	0.41	-0.83	0.05	15.37	<0.005
MCD (nm)[2]	Gt	convex	31.58	28.50	15.06	86.91	116.330	2.03	6.18	10.78	34.16	<0.005
		concave	30.29	28.50	13.45	86.93	135.200	2.45	9.19	11.63	38.38	<0.005
	Hm	convex	49.75	54.00	29.77	90.85	128.830	1.54	3.89	11.35	22.82	<0.005
		concave	63.50	54.02	29.79	90.86	409.180	0.28	-1.43	20.23	31.85	<0.005
AS (Al mol%)[3]	Gt	convex	15.65	14.73	1.69	35.72	67.620	0.83	0.06	8.22	52.55	<0.005
		concave	12.59	12.25	0.18	28.29	25.726	0.24	-0.03	5.07	40.26	0.159
	Hm	convex	12.44	12.87	1.42	17.00	11.470	-0.47	-0.28	3.39	11.47	<0.005
		concave	11.15	12.87	1.43	21.23	15.660	-0.43	0.06	3.96	35.50	<0.005
Content (g kg^{-1})	Gt	convex	13.16	13.09	7.14	23.52	8.820	0.48	0.71	2.97	22.56	0.577
		concave	10.45	10.40	0.60	23.90	14.980	0.26	1.41	3.87	37.06	0.050
	Hm	convex	23.20	23.01	12.92	33.29	14.340	0.18	0.10	3.79	16.32	0.357
		concave	12.39	12.70	0.70	28.60	18.732	0.47	3.37	4.33	34.93	<0.005
SSA (m^2 g^{-1}) [4]	Gt	convex	81.17	82.64	23.74	160.85	527.050	0.07	0.44	22.96	28.28	<0.005
		concave	86.47	82.64	23.73	180.72	746.870	0.38	0.42	27.33	31.61	<0.005
	Hm	convex	36.31	37.04	22.37	61.83	35.276	0.57	1.95	5.94	16.36	0.013
		concave	33.69	32.42	19.16	55.37	76.800	0.37	-0.20	8.76	26.01	0.016
Gt/(Gt+Hm)		convex	0.34	0.34	0.20	0.56	0.005	0.28	-0.05	0.07	20.38	0.640
		concave	0.43	0.43	0.22	0.64	0.006	-0.08	-0.35	0.08	19.03	0.560
Fed (%)[5]		convex	2.45	2.40	1.59	3.22	0.080	0.23	0.46	0.29	11.82	0.010
		concave	1.52	1.55	0.09	3.29	0.220	0.01	3.64	0.47	31.26	0.005

[1]Width at half height (º2θ); [2]Mean crystallite dimension; [3]Aluminium substitution; [4]Specific surface area; [5]Iron extracted by dithionite-citrate-bicarbonate (DCB); [6]SD: Standard deviation; [7]CV: Coefficient of variation; [8]Anderson-Darling statistical test (p>0.05 = normal distribution). Hm: Hematite, Gt: Goethite.

Table 3. Descriptive statistics of the mineral properties [width at half height, mean crystallite size, and Kt/(Kt+Gb) ratio] for the convex and concave areas in the 0.0-0.2 m layer

Statistic	Area	WHH[1]		MCD[2]		Kt/(Kt+Gb)
		Kt	Gb	Kt	Gb	
Mean	Convex	0.760	0.313	14.53	74.47	0.866
	Concave	0.670	0.291	17.42	84.02	0.919
Median	Convex	0.750	0.300	14.44	74.04	0.870
	Concave	0.670	0.285	16.67	85.71	0.923
Minimum	Convex	0.600	0.270	11.39	31.32	0.780
	Concave	0.450	0.270	11.39	44.01	0.830
Maximum	Convex	0.900	0.450	19.73	101.81	0.960
	Concave	0.900	0.375	31.10	101.81	0.957
Variance	Convex	0.008	0.002	5.40	540.28	0.001
	Concave	0.007	0.000	12.14	249.59	0.00065
Asymmetry	Convex	0.070	1.350	0.64	-0.17	-0.01
	Concave	0.080	1.650	1.39	-0.52	-1.20
Kurtosis	Convex	-0.610	1.380	0.02	-1.19	-0.15
	Concave	0.440	3.290	3.39	-0.40	1.56
SD[3]	Convex	0.090	0.050	2.32	23.24	0.04
	Concave	0.086	0.023	3.48	15.80	0.025
CV (%)[4]	Convex	11.500	15.480	16.00	31.21	4.16
	Concave	12.830	8.020	20.00	18.80	2.77
p[5]	Convex	<0.005	<0.005	<0.005	<0.005	0.035
	Concave	<0.005	<0.005	<0.005	<0.005	<0.005

[1]Width at half height (º2θ); [2]Mean crystallite dimension (nm); [3]Standard deviation; [4]Coefficient of variation; [5]Anderson-Darling statistical test (p>0.05 = normal distribution). Kt: Kaolinite, Gb: Gibbsite.

different methods to determine this attribute (Cornell & Schwertmann, 1996).

The distribution of the Gt and Hm contents and the Gt/(Gt+Hm) ratio was normal in the convex area. However, WHH, AS, the Hm and Gt contents, SSA for Gt, Gt/(Gt+Hm), Fe_d, WHH for Kt, MCD for Kt and Gb, and Kt/(Kt+Gb) were all symmetrically distributed with similar means and medians, and near-zero asymmetry and kurtosis - by exception, kurtosis for SSA in hematite was 1.95. The attributes with a normal distribution in the concave area were aluminium substitution in goethite and Gt/(Gt+Hm); on the other hand, WHH, AS, SSA for Gt and Hm, MCD for Gt, Gt/(Gt+Hm), WHH and MCD for Kt all exhibited a symmetric distribution (Tables 2 and 3). The non-normality of the data is not limiting for the use of geostatistics (Cressie, 1991), as long as the distribution is not highly skewed.

Kaolinite had lower coefficients of variation (CVs) than gibbsite (Gb) in the convex area and the opposite was true in the concave area (Table 3). All Gt attributes had higher CVs than those of Hm in both areas, which indicates greater variations in Gt than in Hm. These results are consistent with those reported by Inda Júnior & Kämpf (2005) and Camargo et al. (2008a) for Oxisols. According to Inda Júnior & Kämpf (2005), a smaller variation in hematite properties is a result of an increased specificity of environmental mineral formation factors of goethite, which is more sensitive to environmental changes. The characteristics of goethite and hematite in environments with low Fe content as in the study area are typical of soil populations with high Fe content. This suggests a soil-environmental influence of Fe oxides.

Table 4 shows the Student's *t*-values obtained to assess the difference between the means of the concave area and convex area. The property means, except for WHH, MCD and SSA of Gt, differed significantly at 5 % probability between the concave and convex area.

The higher Gt, Hm and Fe_d values in the convex than the concave area can be ascribed to the higher soil clay content in the former where the A+E horizon was thinner and therefore closer to the clay-richer Bt horizon (Table 1) .

The convex area had the greatest MCD values for all minerals except Hm, and also the highest AS, Hm and Gt contents, and SSA for Hm. On the other hand, in the concave area, the values of WHH and SSA for Gt, MCD for Hm, and the Gt/(Gt+Hm) and Kt/(Kt+Gb) ratios were higher.

The crystallinity of iron oxides depends strongly on soil-environmental factors such as Fe-concentration in the solution, pH, temperature, water activity in the soil and organic matter content (Schwertmann & Taylor, 1989). Based on the differential behaviour of crystallinity (WHH and MCD) in Hm, reflected in the mean values and coefficients of variation (CVs), slope curvature can be assumed to affect the specific interaction of soil-environmental factors that facilitate the formation of Hm. This is consistent with the greater uniformity of the hematite populations in both types of slope curvature. However, the spatial distribution of hematite in curvatures cannot be assessed in terms of means only, but requires the use of CVs and spatial analysis.

The dependence and spatial variability of the attributes in the convex and concave areas was studied via semivariograms of isotropic nature (Figures 2 at 4). In the convex area, the spherical model fitted the MCD data for Hm (110) and Gt (110), WHH for Hm and Gt, aluminium substitution in Hm, the Hm content, SSA for Gt, the Gt/(Gt+Hm) ratio, Fe_d, and MCD for Gb. On the other hand, the exponential model fitted AS for Gt, the Gt content, WHH for Kt and Gb, MCD for Kt, and the Kt/(Kt+Gb) ratio. The pure nugget effect (PNE) was observed only in SSA for Hm. In the concave area, the spherical model fitted MCD for Gt, Gt/(Gt+Hm), WHH for Kt and Kt/(Kt+Gb), whereas the exponential model fitted WHH, AS, the Gt content, SSA for Gt, Fe_d and MCD for Kt. A PNE was observed for MCD, WHH, AS, SSA and content for Hm, and WHH and MCD for Gb.

Of all attributes, only the Gt content in the convex area had a strong spatial dependence [$C_o/(C_o + C_1) < 25$ %], while all others were moderately dependent [$C_o/(C_o + C_1)$ between 25 and 75 %] according to the

Table 4. Mean values of the studied properties in the convex and concave area

Property		Convex area Mean	Concave area Mean	t test
WHH[(1)]	Gt	0.52	0.54	1.51[ns]
	Hm	0.40	0.36	-5.96*
	Kt	0.76	0.67	7.66*
	Gb	0.31	0.29	4.48*
MCD (nm)[(2)]	Gt	31.60	30.30	-0.87[ns]
	Hm	49.70	63.50	6.38*
	Kt	14.53	17.42	-7.11*
	Gb	74.50	84.00	-3.63*
AS (Al mol%)[(3)]	Gt	15.65	12.60	-3.44*
	Hm	12.45	11.15	-2.70*
SSA($m^2\ g^{-1}$)[(4)]	Gt	81.20	86.50	1.60[ns]
	Hm	36.31	33.69	-2.67*
Content ($g\ kg^{-1}$)[(5)]	Gt	13.16	10.44	-5.92*
	Hm	23.20	12.39	-20.03*
Gt/(Gt+Hm)		0.330	0.430	9.47*
Kt/(Kt+Gb)		0.866	0.919	-12.91*

[(1)]Width at half height ($^o2\theta$); [(2)]Mean crystallite dimension; [(3)] Aluminium substitution; [(4)]Specific surface area. [*]and [ns]: significant and not significant at 5 % probability, respectively, by Student's *t*-test. Hm: Hematite, Gt: Goethite, Kt: Kaolinite, Gb: Gibbsite.

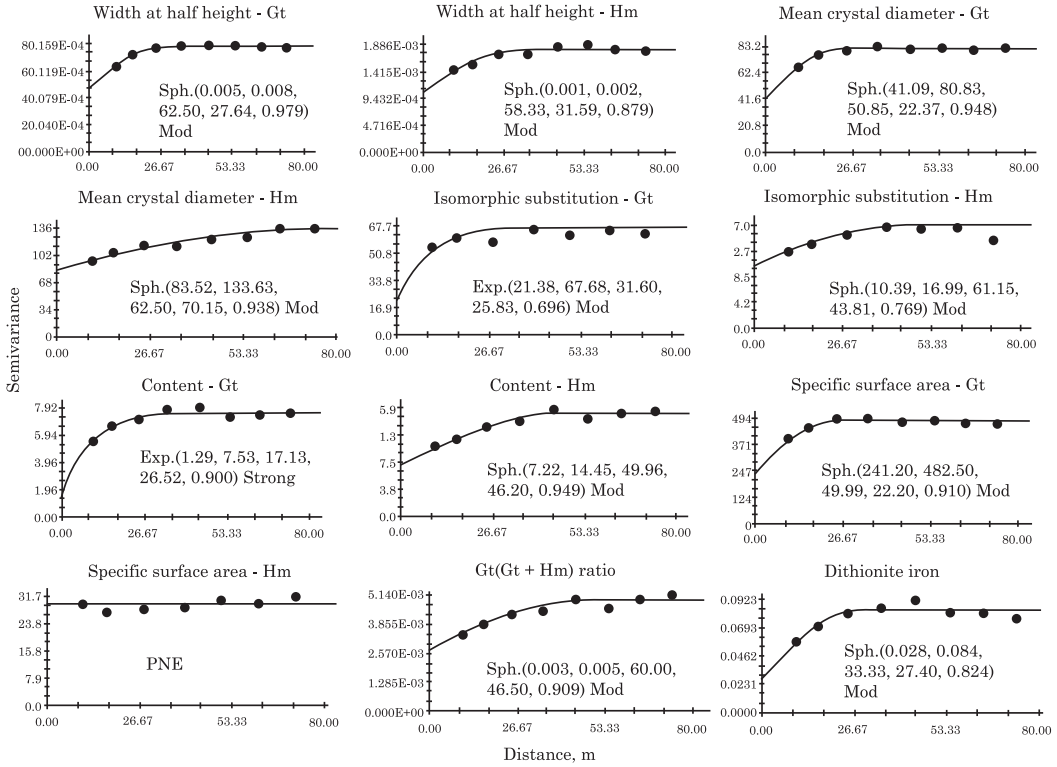

Figure 2. Semivariograms of the studied attributes in the convex area. Gt: goethite, Hm: hematite, PNE: Pure nugget effect, Sph.: Spherical, Exp.: Exponential, Mod: Moderate. Sequence of the semivariogram parameters: C_o; C_1; $C_o/(C_o+C_1)$ (%); range; r^2.

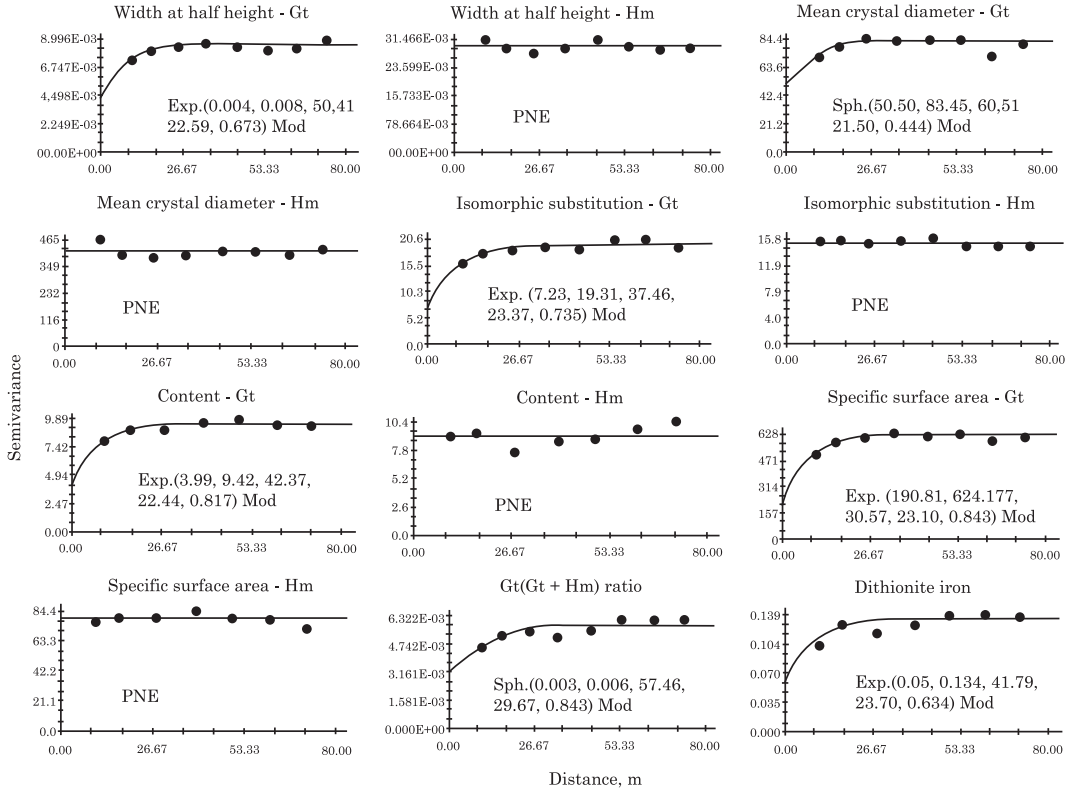

Figure 3. Semivariograms of the studied attributes in the concave area. Gt = goethite, Gt: goethite, Hm: hematite, PNE: Pure nugget effect, Sph.: Spherical, Exp.: Exponential, Mod: Moderate. Sequence of the semivariogram parameters: C_o; C_1; $C_o/(C_o+C_1)$ (%); range; r^2.

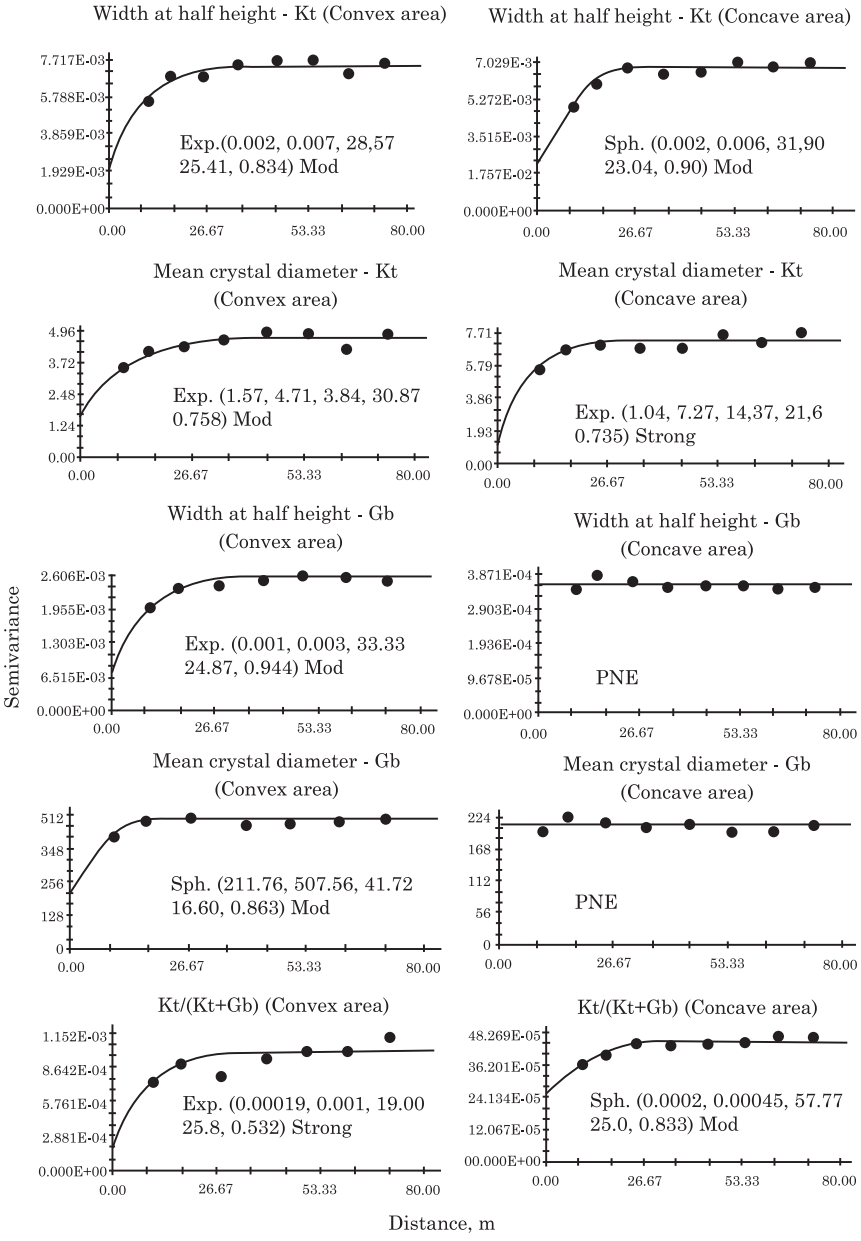

Figure 4. Semivariograms of the studied attributes in the convex and concave areas. Kt: kaolinite, Gb: gibbsite, PNE: Pure nugget effect, Sph.: Spherical, Exp.: Exponential, Mod: Moderate. Sequence of the semivariogram parameters: C_o; C_1; $C_o/(C_o + C_1)$ (%); range; r^2.

classification of Cambardella et al. (2004). In the concave area, MCD, WHH, AS, mineral contents, SSA, Gt/(Gt+Hm) and Fe_d exhibited moderate spatial dependence [$C_o/(C_o + C_1)$ between 25 and 75 %] and MCD for Kt strong dependence.

The ranges for most properties in the convex area were large, which indicates greater continuity in their spatial distribution. This can be ascribed to the more uniform hydraulic conditions of the convex relief facilitating the formation and crystallization of minerals in the clay fraction. Tardy (1993) found the Kt and Gb contents to be correlated with the hydraulic conditions determined by the specific relief. Lucas et al. (1996) found the spatial distribution of secondary minerals such as Kt, Gb and Gt in equatorial regions to be related to the constituents of the soil solution, possibly because the constituting elements in the minerals (e.g. Fe, Si, and Al) were present in the soil solution and the soil phase was markedly affected by weathering processes. According to Duzgoren-Aydin et al. (2002), variations in the nature of minerals of the clay fraction along a profile result from other microenvironmental factors.

In this work, we found different soil-environments of formation of iron oxides and minerals Kt and Gb in the slope curvatures. The spatial continuity in the

concave slope curvature was lower and resulted in a more random interaction pattern of soil-environmental factors. In fact, the number of properties with a pure nugget effect (i.e. a random spatial distribution) was greater in the concave area; this indicates spatially randomness of the pedological processes governing the formation of clay minerals in this area at the studied scale. These results confirm the use of slope curvatures to delimit more uniform areas in the field.

Phenomena such as the adsorption of elements in soil are strongly related to mineral crystallinity. Thus, P tends to be adsorbed by Gt, with low crystallinity and a high SSA, as well as by Gb. This allows the use of the technique described in this study in alternative management practices with a view to minimizing the effects of adsorption on, e.g., soil phosphorus.

CONCLUSIONS

1. Mean crystallite dimension; width at half height for hematite, kaolinite and gibbsite; aluminium substitution; goethite and hematite contents; specific surface area for hematite; and the goethite/(goethite+hematite) ratio differed significantly between slope curvatures.

2. The contents of hematite and goethite were higher in the convex than the concave area; however, hematite predominated in both. Also, hematite had a smaller mean crystallite dimension in the convex area.

3. Kaolinite predominated in the concave area.

4. The properties with spatial dependence in the convex area were mean crystallite dimension; width at half height for hematite, goethite, kaolinite and gibbsite; aluminium substitution; contents and specific surface area for goethite and hematite; and the goethite/(goethite+hematite) and kaolinite/(kaolinite+gibbsite) ratios. In the concave area on the other hand, the properties with spatial dependence were mean crystallite dimension; width at half height for kaolinite and goethite; aluminium substitution; contents and specific surface area for goethite; and the goethite/(goethite+hematite) and kaolinite/(kaolinite+gibbsite) ratios.

5. The spatial variability was lower in the convex area.

ACKNOWLEDGEMENTS

The Usina São Domingos is gratefully acknowledged for access to the study area and the Fundação de Amparo à Pesquisa do Estado de São Paulo (FAPESP) for a postgraduate scholarship to the first author (L.A.C.) and the Conselho Nacional de Desenvolvimento Científico e Tecnológico (CNPq) for Research Grant to the 2nd and 3rd authors.

LITERATURE CITED

BARRÓN, V.; HERRUZO, M. & TORRENT, J. Phosphate adsorption by aluminous hematites of different shapes. Soil Sci. Soc. Am. J., 52:647-651, 1988

BISHOP, T.F.A. & LARK, R.M. The geostatistical analysis of experiments at the landscape-scale. Geoderma, 133:87-106, 2006.

BRITO, L.F.; SOUZA, Z.M.; MONTANARI, R.; MARQUES JR., J.; CAZETTA, D.A.; CALZAVARA, S.A. & OLIVEIRA, L. Influência de formas do relevo em atributos físicos de um Latossolo sob cultivo de cana-de-açúcar. Ci. Rural, 36:1749-1755, 2006.

CAMARGO, L.A.; MARQUES JR, J.; PEREIRA, G.T. & ALLEONI, L.R.F. Spatial correlation between the composition of the clay fraction and contents of available phosphorus of an Oxisol at hillslope scale. Catena, 100:100-106, 2013.

CAMARGO, L.A.; MARQUES JR., J.; PEREIRA, G.T. & HORVAT, R.A. Variabilidade espacial de atributos mineralógicos de um Latossolo sob diferentes formas de relevo. I - Mineralogia da fração argila. R. Bras. Ci. Solo, 32:2269-2277, 2008a.

CAMARGO, L.A.; MARQUES JR., J.; PEREIRA, G.T. & HORVAT, R.A. Variabilidade espacial de atributos mineralógicos de um Latossolo sob diferentes formas do relevo. II - correlação espacial entre mineralogia e agregados. R. Bras. Ci. Solo, 32:2279-2288, 2008b.

CAMBARDELLA, C.A.; MOORMAN, T.B.; NOVAK, J.M.; PARKIN, T.B.; KARLEN, D.L.; TURCO, R.F. & KONOPKA, A.E. Field-scale variability of soil properties in Central Iowa. Soil Sci. Soc. Am. J., 58:1501-1508, 2004.

CAMPOS, M.C.C.; MARQUES JR, J.; PEREIRA, G.T.; MONTANARI, R. & CAMARGO, L.A. Relações solo-paisagem em uma litossequência arenito-basalto na região de Pereira Barreto, SP. R. Bras. Ci. Solo, 31:519-529, 2007.

CASTRO, S.S. Sistemas de transformação pedológica em Marília, SP - B latossólicos e B texturais. São Paulo, Universidade de São Paulo, 1989. 274 p. (Tese de Doutorado)

COELHO, M.R. & VIDAL-TORRADO, P. Caracterização e gênese de perfis plínticos desenvolvidos de arenito do grupo Bauru II – Mineralogia. R. Bras. Ci. Solo, 27:495-507, 2003.

CORNELL, R.M. & SCHWERTMANN, U. The iron oxides. Structure, properties, reactions, occurrence and uses. New York, Weinheim - VHC, 1996. 573p.

CRESSIE, N. Statistics for spatial data. New York, John Wiley, 1991. 900p.

CUNHA, P.; MARQUES JR, J.; CURI, N.; PEREIRA, G.T. & LEPSCH, I.F. Superfícies geomórficas e atributos de Latossolo em uma sequência arenítico-basáltica da região de Jaboticabal (SP). R. Bras. Ci. Solo, 29:81-90, 2005.

CURI, N. & FRANZMEIER, D.P. Toposequence of Oxisols from the Central Plateau of Brazil. Soil Sci. Soc. Am. J., 48:341-346, 1984.

DICK, D.P. Caracterização de óxidos de ferro e adsorção de fósforo na fração argila de horizontes B Latossólicos. Porto Alegre, Universidade Federal do Rio Grande do Sul, 1986. 196p. (Dissertação de Mestrado)

DUZGOREN-AYDIN, N.S.; AYDIN, A. & MALPAS, J. Distribution of clay minerals along a weathered pyroclastic profile, Hong Kong. Catena, 50:17-41, 2002.

FONTES, M.P.F. & WEED, S.B. Iron oxides in selected Brazilian Oxisols: I. Mineralogy. Soil Sci. Soc. Am. J., 55:1143-1149, 1991.

GAMMA DESIGN SOFTWARE. GS+: Geostatistics for the environmental sciences. Plainwell, Gamma Design Software, 1998.

GUALBERTO, V.; RESENDE, M. & CURI, N. Química e mineralogia de Latossolos, com altos teores de ferro, da Amazônia e do Planalto Central. R. Bras. Ci. Solo, 11:245-252, 1987.

INDA JÚNIOR, A.V. & KÄMPF, N. Variabilidade de goethita e hematita via dissolução redutiva em solos de região tropical e subtropical. R. Bras. Ci. Solo, 29:851-866, 2005.

INSTITUTO DE PESQUISAS TECNOLÓGICAS DO ESTADO DE SÃO PAULO - IPT. Mapa geomorfológico do Estado de São Paulo. Escala 1:1.000.000. São Paulo, 1981.

KÄMPF, N. Die Eisenoxidmineralogie einer Klimasequenz von Böden aus Eruptiva in Rio Grande do Sul, Brasilien. Freising, Technische Universität München, 1981.

KÄMPF, N. & CURI, N. Óxidos de ferro: Indicadores de atributos e ambientes pedogênicos e geoquímicos. In: NOVAIS, R.F.; ALVAREZ V., V.H. & SCHAEFER, C.E.G.R., eds. Tópicos em ciência do solo. Viçosa, MG, Sociedade Brasileira de Ciência do Solo, 2000. p.107-138.

KÄMPF, N. & SCHWERTMANN, U. Avaliação da estimativa de substituição de Fe por Al em hematitas de solos. R. Bras. Ci. Solo, 22:209-213, 1998.

KÄMPF, N. & SCHWERTMANN, U. Goethite and hematite in a climosequence in Southern Brazil and their application in classification of kaolinitic Soils. Geoderma, 29:27-39, 1982.

LUCAS, Y.; NAHON, D.; CORNU, S. & EYROLLE, F. Genèse et fonctionnement des sols en milieu equatorial. In: FABRE, F., ed. Géochimie de la surface, pédologie, hydrology. C. R. Acad. Sci., 322:1-16, 1996.

MARQUES JÚNIOR, J. & LEPSCH, I.F. Depósitos superficiais neocenozoicos, superfícies geomórficas e solos em Monte Alto - SP. Geociência, 19:90-106, 2000.

McBRATNEY, A.B.; SANTOS, M.L.M. & MINASNY, B. On digital soil mapping. Geoderma, 117:3-52, 2003.

MEHRA, O.P. & JACKSON, M.L. Iron oxide removal from soils and clay by a dithionite–citrate system buffered with sodium bicarbonate. Clays Clay Miner., 7:317-327, 1960.

MINITAB, Release. Making data analysis easier: Version 13.1, 2000.

MONIZ, A.C. & BUOL, S.W. Formation of an Oxisol-Ultisol transition in São Paulo - Brazil. I. Double-water flow model of soil development. Soil Sci. Soc. Am. J., 46:1228-1233, 1982.

NORRISH, K. & TAYLOR, R.M. The isomorphous replacement of iron by aluminum in soil goethites. J. Soil Sci., 12:294-306, 1961.

OLIVEIRA JUNIOR, J.C.; SOUZA, L.C.P.; MELO, V.F. & ROCHA, H.O. Variabilidade espacial de atributos mineralógicos de solos da formação Guabirotuba, Curitiba (PR). R. Bras. Ci. Solo, 35:1481-1490, 2011.

PEÑA, F. & TORRENT, J. Relationship between phosphate sorption and iron oxides in Alfisols from a river terrace sequence of Mediterranean Spain. Geoderma, 33:283-296, 1984.

PENNOCK, D.J. & VELDKAMP, A. Advances in landscape-scale soil research. Geoderma, 133:1-5, 2006.

REATTO, A.; BRUAND, A.; MARTINS, E.S.; MULLER, F.; SILVA, E.M.; CARVALHO JR, O.A. & BROSSARD, M. Variation of the kaolinite and gibbsite content at regional and local scale in Latosols of the Brazilian Central Plateau. C. R. Geosci., 340:741-748, 2008.

SCHULZE, D.G. & SCHWERTMANN, U. The influence of aluminium on iron oxides: X. Properties of Al-substituted goethites. Clay Miner., 19:521-539, 1984.

SCHULZE, D.G. The influence of aluminium on iron oxides VIII. Unit-cell dimension of Al-substituted goethites and estimation of Al from them. Clays Clay Miner., 32:36-44, 1984.

SCHWERTMANN, U. The effect of pedogenic environments on iron oxide minerals. In: STEWART, B.A., ed. Advances in soil science. New York, Springer Verlag, 1985. p.171-200.

SCHWERTMANN, U. Solubility and dissolution of iron oxides. In: CHEN, Y. & HADAR, Y., eds. Iron nutrition and interactions in plants. Dordrecht, Kluwer Academic, 1991. p.3-27.

SCHWERTMANN, U. & FISCHER, W.R. Zur Bildung von a-FeOOH und a-Fe2O3 aus amorphem Eisen(III)-hydroxid. III. Z. Anorg. Allgem. Chem., 346:137-142, 1966.

SCHWERTMANN, U.; FITZPATRICK, R.W.; TAYLOR, R.M. & LEWIS, D.G. The influence of aluminium on iron oxides. Part II: Preparation and properties of Al-substituted hematites. Clays Clay Miner., 27:105-12, 1979.

SCHWERTMANN, U. & CARLSON, L. Aluminium influence on iron oxides: XVII. Unit-cell parameters and aluminium substitution of natural goethites. Soil Sci. Soc. Am. J., 58:256-261, 1994.

SCHWERTMANN, U. & KÄMPF, N. Properties of goethite and hematite in kaolinitic soils of southern and central Brazil. Soil Sci., 139:344-350, 1985.

SCHWERTMANN, U. & MURAD, E. Effect of pH on the formation of goethite and hematite from ferrihydrite. Clays Clay Miner., 31:277-284, 1983.

SCHWERTMANN, U. & TAYLOR, R.M. Iron oxides. In: DIXON, J.B. & WEED, S.B., ed. Minerals in soil environments. 2.ed. Madison, SSSA, 1989. p.379-438. (Book Series, 1)

SINGER, A.; SCHWERTMANN, U. & FRIEDL, J. Iron oxide mineralogy of Terre Rosse and Rendzinas in relation to their moisture and temperature regimes. Eur. J. Soil Sci., 49:385- 395, 1998.

SOIL SURVEY STAFF. Soil Taxonomy: A basic system of soil classification for making and interpreting soil surveys. 2.ed. Washington, 1999. 869p.

SOUZA, Z.M.; MARQUES JR, J.; PEREIRA, G.T. & BARBIERI, D.M. Small relief shape variations influence spatial variability of soil chemical attributes. Sci. Agric., 63:161-168, 2006.

SUGUIO, K. Calcretes of the Bauru Group (Cretaceous), Brazil: petrology and geological significance. São Paulo, Universidade de São Paulo, 1973. 236 p. (Tese de Doutorado)

TARDY, Y. Pétrologie des latérites et des sols tropicaux. Paris, Masson, 1993. 459p.

TORRENT, J.; BARRÓN, V. & SCHWERTMANN, U. Phosphate adsorption and desorption by goethites differing in crystal morphology. Soil Sci. Soc. Am. J., 54:1007-1012, 1990.

TORRENT, J.; GUZMAN, R. & PARRA, M.A. Influence of relative humidity on the crystallization of Fe (III) oxides from ferrihydrite. Clays Clay Miner., 30:337-340, 1982.

TORRENT, J.; SCHWERTMANN, U. & BARRON, V. The reductive dissolution of synthetic goethite and hematite in dithionite. Clay Miner., 22:329-337, 1987.

TRANGMAR, B.B.; YOST, R.S. & UEHARA, G. Application of geostatistics to spatial studies of soil properties. Adv. Agron., 38:54-94, 1985.

TROEH, F.R. Landform equations fitted to contour maps. Am. J. Sci., 263:616-627, 1965.

VIEIRA, S.R. Geoestatística em estudos de variabilidade espacial do solo. In: NOVAIS, R.F.; ALVAREZ V., V.H. & SCHAEFER, G.R., eds. Tópicos em ciência do solo. Viçosa, MG, Sociedade Brasileira de Ciência do Solo, 2000. p.1-54.

WILSON, M.A.; SCHOENEBERGER, P.J.; WEST, L. & GRAHAM, R.C. Distribution of soil mineral in landscapes. Geoderma, 154:417, 2010.

WIRIYAKITNATEEKUL, W.; SUDDHIPRAKARN, A.; KHEORUENROMNE, I.; MIRK, M.N.S. & GILKES, R.J. Iron oxides in tropical soils on various parent materials. Clay Miner., 42:437-451, 2007.